JACS
JOURNAL OF THE AMERICAN CHEMICAL SOCIETY

ARTICLE

pubs.acs.org/JACS

Computational Study of the Effect of Confinement within Microporous Structures on the Activity and Selectivity of Metallocene Catalysts for Ethylene Oligomerization

Hervé Toulhoat,*[,†] Mireille Lontsi Fomena,[‡] and Theodorus de Bruin[‡]

[†]Direction Scientifique and [‡]Direction Chimie et Physico-chimie Appliquées, IFP Energies nouvelles, 1 et 4 avenue de Bois-Préau, 92852 Rueil-Malmaison, France

Supporting Information

ABSTRACT: The effect of confinement within some zeolitic structures on the activity and selectivity of metallocene catalysts for the ethylene oligomerization has been investigated using grand canonical Monte Carlo simulations (GCMC). The following zeolite (host) frameworks displaying different pore sizes, have been studied as solid hosts: mazzite (MAZ), AIPO-8 (AET), UTD-1F (DON), faujasite (FAU), and VPI-5 (VFI). Intermediates and transition states involved in the ethylene trimerization reaction catalyzed by a Ti-based catalyst [(η^5-$C_5H_4CMe_2C_6H_5$)$TiCl_3$/MAO] have been used as sorbates (guests). We have demonstrated linear correlations with slope $a_{H,j}$ between the adsorption enthalpy and the molecular volume V_m of the sorbates, each holding for a given microporous host below a host-specific threshold $V_{mmax,j}$. Beyond this maximal molecular volume, the adsorption vanishes due to steric exclusion. $a_{H,j}$ increases, and $V_{mmax,j}$ decreases with decreasing host pore size, in line with the confinement concept. We moreover showed that, in the limit of vanishing loading (Henry regime), the enthalpies and entropies of adsorption in a given host are linearly correlated. We have defined a host-specific confinement compensation temperature a_j, which refers to a temperature where the stabilizing adsorption enthalpic interactions are canceled out against the loss in entropy. However, calculated a_j are much larger than the operating temperatures. With a setup microkinetic model, we predict that the activity and selectivity of the confined Ti-catalyst in ethylene oligomerization can be significantly altered with respect to homogeneous phase conditions, since the adsorption free energies of transition states and intermediates also become functions of $a_{H,j}$ and V_m. We have applied this theory to predict the optimum host pore size to get maximum α-octene production, instead of α-hexene, which is primarily produced in the homogeneous phase. We also predict a significantly increased activity for confined catalysts.

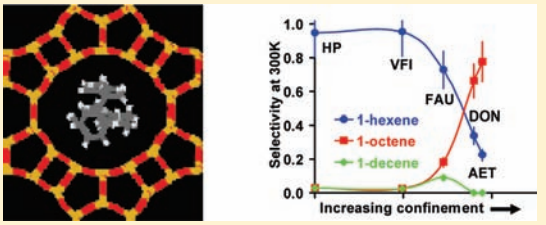

1. INTRODUCTION

In search of the advantages of "single site catalysis" expected from homogeneous catalysts, namely, higher specific activities and targeted selectivities, over their heterogeneous counterparts, allied to the advantages of the latter, mostly an easy separation from the products, numerous studies have been already devoted to immobilizing techniques of molecular or enzymatic catalysts by chemical or electrostatic grafting and adsorption.[1−6]

However, there are no reports of industrial processes that favorably combine the activity and selectivity of molecular catalysts and the implementing benefits as experienced for heterogeneous catalysts.

The disturbance brought to catalytic molecular species by a specific interaction with a solid surface is usually deactivating.[7] The surface sites often behave as strong coordinating metallic center ligands. However, the development attempts in supported organometallic catalysis are principally focused on the chemical anchoring, rather than on confinement effects.

Here, confinement refers to the nonspecific adsorption of a molecular species within a pore or cavity, the curvature radius of which is slightly larger than that of the adsorbed molecular species. Nonspecific adsorption is mainly driven by favorable van der Waals interactions between the sorbate and the pore walls. For a given pore radius, the confinement in micropores induces a stabilization that increases with the molecular size, as the average distance between atoms belonging to the sorbate and those belonging to the pore walls decreases, until a critical size. Beyond that specific size, repulsive forces arising from the Pauli principle overcome the attractive dispersion (London−Heitler) forces (steric constraint), so that the enthalpic component of the free energy of sorbate−host interaction cooperates with the entropic component to prevent adsorption.[8]

In the present computational study we explore this concept to investigate if the activity and selectivity of a molecularly catalyzed reaction can be modified. For example, Ti-based catalysts can be applied to selectively trimerize ethene into α-hexene.[9] It has recently been shown that the selectivity of this reaction is

Received: July 6, 2010
Published: February 8, 2011

dx.doi.org/10.1021/ja105950z | J. Am. Chem. Soc. 2011, 133, 2481–2491

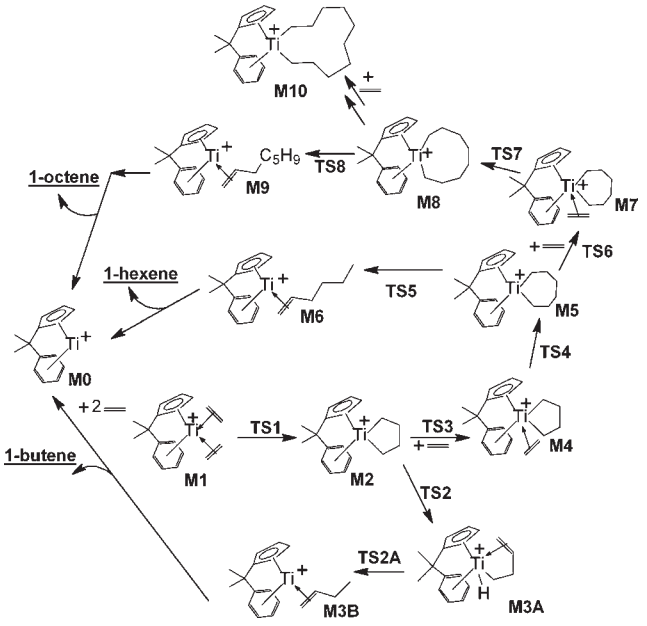

Figure 1. Reaction paths for ethene oligomerization by metallacycle growth using a Ti-based catalyst.

determined by two competitive reaction pathways:[10] the ring-opening reaction of the titana(IV) cycloheptane leading to α-hexene and the insertion of a fourth ethylene molecule into that titana(IV) cycloheptane conducting to α-octene. Figure 1 shows the schematic reaction pathways of ethene oligomerization on Ti-catalyst by metallacycle growth. By performing this reaction in microporous structures with adapted pore size, large-size intermediates, that is, those who eventually lead to α-octene or even α-decene, could be more stabilized as a result of confinement than smaller-sized ones, thereby interestingly shifting the selectivity from α-hexene to higher order olefins (α-octene or α-decene). By the same token, the activity is also expected to increase in some conditions.

By the use of grand canonical Monte Carlo (GCMC) calculations, we will show that the activity and selectivity of the reaction outcome can indeed be altered. For that purpose, we have calculated the adsorption energies and entropies in the Henry regime, for the previously identified reaction intermediates[10−12] for oligomer formation using Ti-based catalysts, in representative microporous structures with increasing pore sizes. We have then developed a microkinetic model to account for confinement effects on the activity and selectivity. Using the thermodynamic parameters characterizing the confinement effect determined for a choice of microporous guests, we predict the optimal window and temperature to shift the selectivity from of α-hexene to α-octene. Moreover, we predict confinement induced activity amplifications, as a function of temperature and host characteristics.

2. THEORY

2.1. Henry Constant, Adsorption Enthalpy, and Entropy. Henry's law states that "at a constant temperature, the amount of a given gas in a given volume of liquid to form an ideal mixture is proportional to the partial pressure of that gas in equilibrium with that liquid".[13] To transpose this law to the adsorption domain, it can be said that when an adsorbent is in equilibrium with a reservoir containing a given component, the loading (Γ) of this component in the adsorbent is proportional to the fugacity (f) of the component in the reservoir in the limit of zero pressure, that is, at low coverage:

$$K_H = \lim_{f \to 0} \frac{\Gamma(f)}{f} = \frac{N}{fV_{uc}} \quad (1)$$

where V_{uc} is the free volume of the adsorbent unit cell, N the amount adsorbed per unit cell, and K_H the Henry constant.

Since, at low coverage, the adsorption equilibrium and thus the Henry constant only depends on the interaction of a single molecule with the adsorbent, the investigation of its temperature dependence provides access to an understanding of essential thermodynamics properties such as adsorption enthalpy (ΔH_{ads}) and entropy (ΔS_{ads}).[14]

At low coverage, Henry's constant is directly correlated to the Gibbs free energy of adsorption (ΔG_{ads})[14] according to:

$$K_H = \frac{1}{k_B T} \exp\left(\frac{-\Delta G_{ads}}{RT}\right) \quad (2)$$

$$\text{with} \quad \Delta G_{ads} = \Delta H_{ads} - T\Delta S_{ads} \quad (\text{in kcal}\cdot\text{mol}^{-1}) \quad (3)$$

Note that R is the ideal gas constant, k_B the Boltzmann constant, and T corresponds to the temperature expressed in Kelvin.

It can thus easily be seen that, in the limit of zero fugacity, the adsorption enthalpies (ΔH_{ads}) and entropies (ΔS_{ads}) can be evaluated from respectively the slope and the Y-axis intercept by plotting the logarithm of $k_B T$ times the Henry constant as a function of the reciprocal of temperature ($1/T$):

$$\ln(k_B T K_H) = -\frac{\Delta H_{ads}}{RT} + \frac{\Delta S_{ads}}{R} \quad (4)$$

2.2. Compensation Effect. Introduced by Constable for the first time in 1923, the compensation effect describes from a general point of view, the occurrence of a linear relationship between enthalpy and entropy changes otherwise associated to the same change in free energy.[15−17]

In the case of adsorption, this phenomenon can be physically understood by a loss in entropy (reduction of freedom of motion, negative ΔS_{ads}), that is compensated by a gain in enthalpy (binding energy, negative ΔH_{ads}).[15,17] The variation of adsorption enthalpies and entropies thus share the same sign. The postulated linear relationship may be expressed as the following equation:

$$\Delta H_{ads} = a\Delta S_{ads} + b \quad (5)$$

where the slope a (with dimension of temperature) may be called the confinement compensation temperature, while constant b has the dimension of energy.

2.3. Linear Relationships between the Molecular Volume of Sorbates and Their Enthalpy and Entropy of Adsorption. In what follows, we introduce our central assumptions regarding the confinement effect, namely, the occurrence of linear relationships between the enthalpies and the entropies of adsorption of adsorbates in a given microporous host, identified by subscript j, and their molecular volume V_m in eqs 6 and 7. The molecular volume is defined as the volume delineated by the envelope surface of the van der Waals spheres, centered on atomic cores belonging to the molecule in its geometry in the ground state.

Equations 6 and 7 hold as long as repulsive forces arising from the Pauli principle (steric constraint) do not overcome the attractive dispersion (London−Heitler) forces. If they do, the enthalpic component of the free energy of sorbate−host interaction cooperates with the entropic component to prevent adsorption. For a given host and pore size, one expects therefore to find a maximal molecular volume $V_{\mathrm{mmax},j}$ beyond which the adsorption free energy components vanish.[24] We have chosen to describe the confinement effect with molecular volume because in our opinion it is more insightful with respect to the molecular sieving problem and also since we introduced earlier in a similar approach[24] the cubic root of the relative molecular volumes as a scaling factor representing an average molecular diameter, to be compared with the pore diameter. However, we do not claim that the correlation for the molecular volume is better than with another closely correlated descriptor.

$$-\Delta H_{\mathrm{ads},j} = a_{H,j}V_{\mathrm{m}} + b_{H,j} \qquad 0 \le V_{\mathrm{m}} \le V_{\mathrm{mmax},j} \quad (6)$$

$$-\Delta S_{\mathrm{ads},j} = a_{S,j}V_{\mathrm{m}} + b_{S,j} \qquad 0 \le V_{\mathrm{m}} \le V_{\mathrm{mmax},j} \quad (7)$$

From eq 3, it follows, in the same interval of V_{m} as above:

$$-\Delta G_{\mathrm{ads},j} = a_{G,j}V_{\mathrm{m}} + b_{G,j} \quad (8)$$

with (see Supporting Information):

$$a_{G,j} = a_{H,j} - Ta_{S,j} \quad (9)$$

$$b_{G,j} = b_{H,j} - Tb_{S,j} \quad (10)$$

Furthermore, when a compensation effect occurs, and assuming that a and b in eq 5 are host-dependent and therefore indexed by subscript j,

$$a_{G,j} = a_{H,j}\left(1 - \frac{T}{a_j}\right) \quad (11)$$

$$b_{G,j} = b_{H,j}\left(1 - \frac{T}{a_j}\right) + b_j\frac{T}{a_j} \quad (12)$$

Besides, by eliminating V_{m} from eq 7 into eq 6, one obtains:

$$\Delta H_{\mathrm{ads},j} = \left(\frac{a_{H,j}}{a_{S,j}}\right)\Delta S_{\mathrm{ads},j} + \frac{a_{H,j}b_{S,j}}{a_{S,j}} - b_{H,j} \quad (13)$$

which shows that our assumptions in eq 6 and 7 imply a compensation effect, for which the confinement compensation temperature is:

$$a_j = \frac{a_{H,j}}{a_{S,j}} \quad (14)$$

Since no attractive or repulsive adsorption forces can be expected as the molecular volume vanishes, we expect further to have:

$$b_{H,j} = 0 \quad (15)$$

As a consequence, from eqs 12 and 13 we deduce:

$$b_j = b_{G,j}\frac{a_{H,j}}{a_{S,j}T} \quad (16)$$

Equation 16 or 12 imply that $b_{G,j}$ is proportional to the absolute temperature T.

Notice that the physical meaning of the confinement compensation temperature appears clearly from eq 11, since at this temperature $a_{G,j} = 0$, and therefore from eq 8, the influence of confinement on adsorption in host j becomes independent of the molecular volume. Above this host-dependent confinement compensation temperature, increasing molecular volumes will have an unfavorable effect on adsorption in the considered host, while the favorable effect will be observed only below this temperature.

2.4. Kinetic Modeling of the Effect of Confinement on Oligomerization Activity and Selectivity. According to Eyring, a reaction rate constant can be expressed by:

$$\nu = \frac{k_{\mathrm{B}}\mathrm{T}}{h}\exp\left(-\frac{\Delta G^{\pm}}{RT}\right) \quad (17)$$

where h is Planck's constant and $\Delta G^{\pm}$ the Gibbs free activation energy of the considered elementary step.[18]

Assuming that the overall rate of oligomerization is of first order with respect to ethene pressure, following Hagen's experimental finding[25] in the homogeneous phase with the Teuben catalyst, this overall rate of oligomerization $r_{\mathrm{rds},j}$, now catalyzed in confinement in host j, may be expressed as:

$$r_{\mathrm{rds},j} = \frac{k_{\mathrm{B}}\mathrm{T}}{h}\exp\left(-\frac{\Delta G^{\pm}_{\mathrm{rds},j}}{RT}\right)P_{\mathrm{C_2H_4}}\exp\left(-\frac{\Delta G^{\mathrm{C_2H_4}}_{\mathrm{ads},j}}{RT}\right) \quad (18)$$

where $\Delta G^{\mathrm{C_2H_4}}_{\mathrm{ads},j}$ stands for the adsorption free energy of ethene in host j, $P_{\mathrm{C_2H_4}}$ for the partial pressure of ethene in j and $\Delta G^{\pm}_{\mathrm{rds},j}$ for the free energy of activation of the rate determining step (rds) in host j. Notice that the rds may change with confinement and temperature.

The adsorption free energy can be expressed as:

$$\Delta G^{i}_{\mathrm{ads},j} = G^{i}_{j} - G^{i}_{0} \quad (19)$$

where G^{i}_{j} corresponds to the free energy of the adsorbed species i of molecular volume $V_{\mathrm{m},i}$ confined in host j that is characterized by the parameters $a_{G,j}$ and $b_{G,j}$, and G^{i}_{0} is the free energy of species i in the surrounding homogeneous phase (reservoir) at a given temperature and pressure.

It was shown on the basis of density functional theory (DFT) calculations, by our group[10] and independently by Tobisch and Ziegler,[12] that the overall rate determining step for metallacyclic oligomerization of ethene in homogeneous phase catalyzed by the Teuben system, is the growth from the five-membered metallacyclic intermediate (M2) to the seven-membered M5 ring structure, via the transition states TS3 and TS4 (see Figure 1). This step has an overall free energy barrier of 23.3 kcal/mol at 298.15 K. The β-elimination from M2 leading to the product α-butene and restoring the uncoordinated complex M0 is disfavored, with a free energy barrier of 25.9 kcal/mol at 298.15 K. From the common intermediate M5, either α-hexene is produced by β-elimination via the transition state TS5 (free energy barrier of 18.4 kcal/mol at 298.15 K), or further growth occurs by addition of one ethene leading to the nine-membered M8 via TS7 (free energy barrier of 24.2 kcal/mol at 298.15 K), the latter pathway thus being disfavored in the homogeneous phase.

From a more general point of view, and changing slightly the notation of intermediates and transition states with respect to

dx.doi.org/10.1021/ja105950z | J. Am. Chem. Soc. 2011, 133, 2481–2491

Figure 1 and ref 10 for an easier formulation, metallacyclic catalytic oligomerization presents serial growth steps, by addition of one ethene to a $(2N+1)$ membered metallacycle $M(2N+1)$, each competing with a termination steps by β-elimination leading to opening of this intermediate and production of the corresponding α-olefinic $2N$ mer. At steady-state, the distribution of $2N$ mers will be governed by the Boltzmann factors involved in the rate constants of each step, therefore by the corresponding free energy barriers. We have seen above how the distinctive trimerization selectivity $(N = 3)$ of the Teuben catalyst is determined in homogeneous phase. Since β-elimination steps do not involve a significant change of molecular volume between the initial intermediates and the transition states, the corresponding free energy barriers will not be significantly affected by the confinement effect. In contrast, all growth steps involve a change of molecular volume at the transition state by ca. 40 $Å^3$ upon insertion of one ethene. Therefore a relative stabilization by confinement of the transition state with respect to the preceding intermediate, in other terms a lowering of the free energy barrier, is expected. Hence, confinement favors all growth steps, until N_{max}, the molecular volume of the transition state for further ethene insertion from the $(2N_{max}+1)$ membered metallacycle exceeds $V_{mmax,j}$: the host j will then stop further growth by steric exclusion, as if the corresponding free energy barrier for insertion becomes infinite.

We obtain further, making use of eq 8, the following simple connections between free energy barriers for reaction in homogeneous phase and confined environment (details of the derivation can be found in Supporting Information):

$$\Delta G^{\pm,\mathrm{exp}}_{2N,j} = \Delta G^{\pm,\mathrm{exp}}_{2N,0} - a_{G,j}\left(V_{\mathrm{m},TS(2N)} - V_{\mathrm{m},M(2N-1)}\right) \quad (20)$$

$$\Delta G^{\pm,\mathrm{BHT}}_{2N-1,j} = \Delta G^{\pm,\mathrm{BHT}}_{2N-1,0} - a_{G,j}\left(V_{\mathrm{m},TS(2N-1)el} - V_{\mathrm{m},M(2N-1)}\right) \approx \Delta G^{\pm,\mathrm{BHT}}_{2N-1,0} \quad (21)$$

Then, according to eq 17 the ratio of rate constants in a confined environment of host j over the homogeneous phase is for an expansion step of rank $2N$:

$$\rho_{2N,j} = \frac{\upsilon_{2N,j}}{\upsilon_{2N,0}} = \exp\left[\frac{a_{G,j}\left(V_{\mathrm{m},TS(2N)} - V_{m,M(2N-1)}\right)}{RT}\right] \quad (22)$$

This equation shows that, as discussed above, the confinement induced acceleration of a given step only depends on the coefficient $a_{G,j}$ and on the increment of molecular volumes between initial and transition states. As a consequence, the rate determining step along the oligomerization main pathway might also change under confinement and thus has to be determined for each particular host.

In a first approximation, the temperature dependence of any $\Delta G^{\pm,\mathrm{EXP}}_{2N,0}$ or $\Delta G^{\pm,\mathrm{BHT}}_{2N-1,0}$ can be represented by a linear expansion and can be written as:

$$\Delta G^{\pm,\mathrm{exp}}_{2N,0} = C_{2N}T + D_{2N} \quad (23)$$

where C_{2N} and D_{2N} are constants and T is the temperature in Kelvin (similarly for β-elimination barriers).

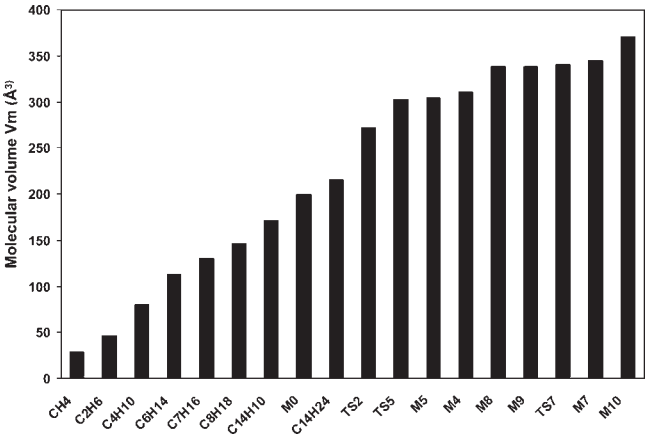

Figure 2. Calculated molecular volume for neutral hydrocarbons, intermediates, and transition states adsorbates, with $C_{14}H_{10}$: phenanthrene and $C_{14}H_{24}$: perhydrophenanthrene.

With $r_{2N,j}$ being the rate of production of a given α-olefinic $2N$ mer catalyzed in confinement in host j, the total productivity rate $r_{\mathrm{tot},j}$ is:

$$r_{\mathrm{tot},j} = \sum_{N=3}^{N=N_{\max}} r_{2N,j} \quad (24)$$

and the selectivity in $2N$ mer is:

$$S_{2N,j} = \frac{r_{2N,j}}{r_{\mathrm{tot},j}} = \frac{r_{2N,j}}{\sum_{N=3}^{N=N_{\max}} r_{2N,j}} \quad (25)$$

Each rate $r_{2N,j}$ may be expressed by an equation similar to eq 18, where $\Delta G^{\pm}_{\mathrm{rds},j}$ now stands for the free energy barrier to the rate determining step along the corresponding particular termination pathway. With that, we assume an order one with respect to ethene for the production of all $2N$ mers, on the basis of the experiment (as seen above for $N = 3$ in homogeneous phase) and since each growth step involves the insertion of a single ethene molecule. With eqs 18, 20, 21, and 25 selectivities are now determined. Further considerations are reported in Supporting Information.

3. MODELS AND COMPUTATIONAL DETAILS

3.1. Models. Adsorption equilibria were simulated for a series of hydrocarbons and metallacyclic intermediates and transition states with increasing molecular volume (M0 to M10) as depicted in Figure 2. The geometries of these molecular models result from our previous DFT calculations, as reported online in Supporting Information of the corresponding article.[10]

In total five zeolitic frameworks have been considered as adsorbents: mazzite (MAZ), AlPO-8 (AET framework type), UTD-1F (DON framework type), faujasite (FAU), and VPI-5 (VFI framework type) (Figure 3), and their pore diameters (longest oxygen−oxygen interatomic distance) vary from 10.1 Å (MAZ) to 15.4 Å (VFI).[19] Different supercells have been constructed (Table 1) that were used in the Monte Carlo simulations.

3.2. Computational Details. GCMC simulations, in which the chemical potential μ, volume V, and temperature T are constant,[20] combined with the configurational bias Monte Carlo algorithm (CBMC)[21] as implemented in Materials Studio's Sorption module,[22] have been performed. Henry constants (K_H) were typically calculated

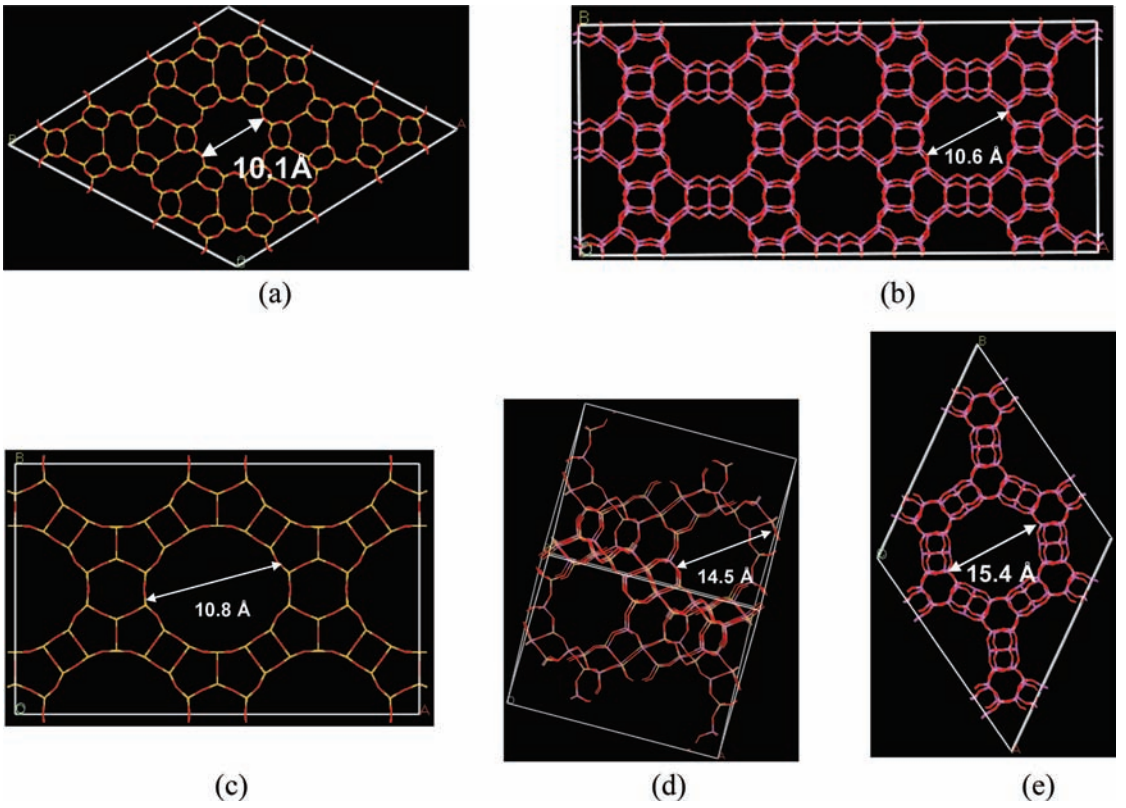

Figure 3. Principal pore diameters (longest oxygen−oxygen interatomic distance) of the microporous frameworks: (a) MAZ, (b) AET, (c) DON, (d) FAU, and (e) VFI.

Table 1. Supercell and Volume of Microporous Frameworks Used

microporous frameworks	supercell used	unit cell volume (Å^3)
mazzite (MAZ)	2 × 2 × 4	2239.86
aluminophosphate (AET)	2 × 2 × 4	4057.16
UTD-1F (DON)	2 × 1 × 3	3737.92
faujasite (FAU)	1 × 1 × 1	15677.6
VPI-5 (VFI)	2 × 2 × 4	4057.16

using 100 million steps, over a temperature range from 577 to 298 K and a temperature step size of 2.8 K.[23] In our calculations both the zeolitic frameworks and the inserted species were treated as rigid bodies. Consequently, we anticipate that the major changes in entropy and enthalpy are of translational and rotational character.

The universal force field (UFF) was applied with a convergence criterion of 4.19 × 10^{-6} kJ/mol for the energy calculation and a cutoff radius of 18.5 Å for the van der Waals interactions. We have used UFF because it covers all elements involved in our test case, the oligomerization catalyzed by a Ti-based organometallic complex, in contrast to more recent force fields of probably better accuracy for adsorption of hydrocarbons in zeolites. In this work, we are not primarily concerned by accuracy in reproducing experimental adsorption isotherms, but rather by consistent qualitative and relative trends. We had used UFF also in our previous work,[24] in the same spirit, with good results.

Note that energy contributions from electrostatic interactions have been ignored. In test calculations, we have introduced electrostatic interactions, in particular we have run GCMC calculations with guests bearing one plus charge (the Ti Teuben complex is actually active in a cationic form, compensated by the negative MAO ion as cocatalyst), compensated by one minus background charge distributed over the framework. The associated electrostatic free energy introduces a small (< 5 kcal/mol) stabilizing contribution to the free enthalpy that slightly depends on the microporous framework structure. However, it is independent of the molecular volume of the guest, as expected. A more accurate evaluation of the contribution of electrostatic interactions will arise from the results of ongoing QM/MM calculations, which involve electronic embedding. Preliminary results do not change the trend already described by the simple force field approximation.

As mentioned above, the gas phase-optimized reaction intermediates and their corresponding energies have been taken from De Bruin et al.[10] Gibbs free energy values (G_0^i) have been calculated at temperatures from 300 to 600 K with an interval of 50 K at a pressure of 1 atm.

4. RESULTS AND DISCUSSION

4.1. Henry Constant Calculation: From Adsorption Energy to Gibbs Free Energy. Using the computed Henry constants, adsorption enthalpies and entropies have been calculated. $-\Delta H_{ads}$ has been plotted as function of the molecular volume of the inserted species for the five adsorbents considered in Figure 4. Linear correlations are observed for all solids, with regression coefficients better than 0.99. The steepness of the slope, $a_{H,j}$, is, however, determined by the adsorbent j, or more precisely, the geometry and the size of the pore. Steeper slopes are observed for relatively small pore sizes, while larger pores display smaller slopes. Pores with infinite size—corresponding to a homogeneous phase—have slope zero. It is also remarked that for MAZ, which has a relatively small pore size, only species with a molecular volume of up to 250 Å^3 can be inserted; above this volume ($V_{max,MAZ}$), they are rejected because of repulsive host−guest interactions.

dx.doi.org/10.1021/ja105950z |J. Am. Chem. Soc. 2011, 133, 2481–2491

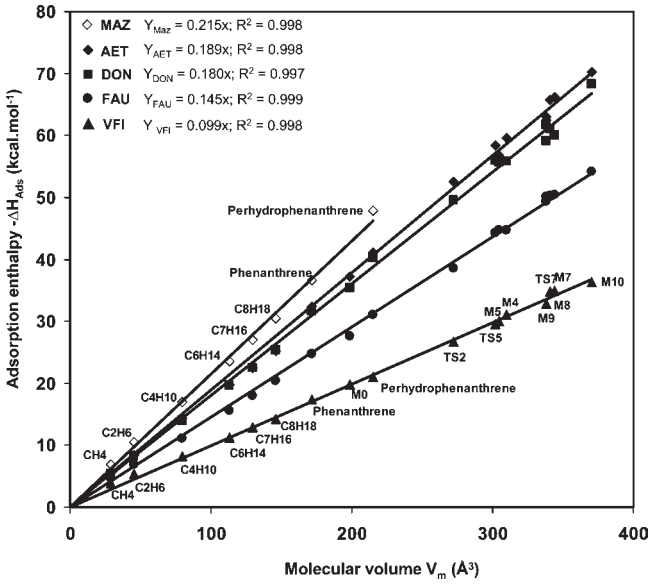

Figure 4. Calculated adsorption enthalpies as function of the molecular volume of the inserted species within the microporous structures: MAZ, AET, DON, FAU, and VFI.

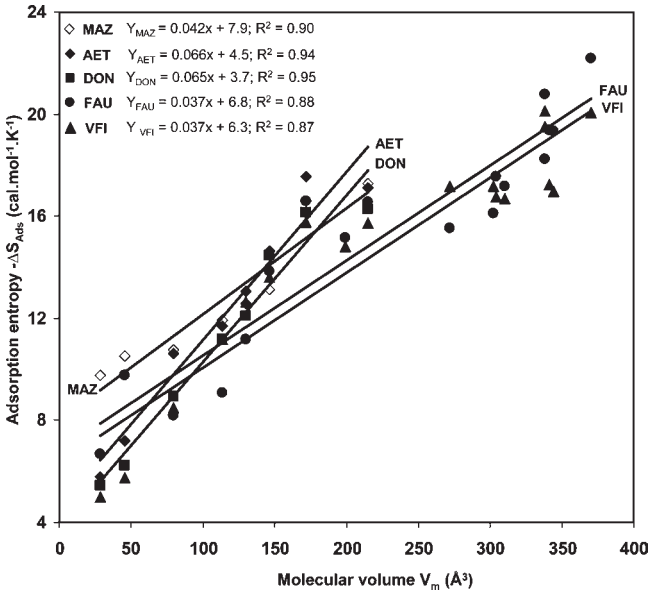

Figure 5. Calculated adsorption entropies as function of the molecular volume of the inserted species within the microporous structures: MAZ, AET, DON, FAU, and VFI.

While the adsorption reactions are exothermic, they are (partially) counterbalanced by the calculated negative adsorption entropy, as can been seen from Figure 5, where $-\Delta S_{ads}$ has been plotted against molecular volume (V_m) of the inserted species for the investigated frameworks. We have experienced that the calculated ΔS_{ads} values are more prone to statistical errors than ΔH_{ads}, especially for particles with a molecular volume that approaches the available volume of the host. We have therefore added small hydrocarbon compounds, which easily insert, to improve statistics to better reveal the linear relationship between V_m and ΔS_{ads}. From Figure 5 it is seen that all slopes are positive and steeper for the microporous structures with smaller pore sizes DON and AET, as compared to for example FAU or VFI.

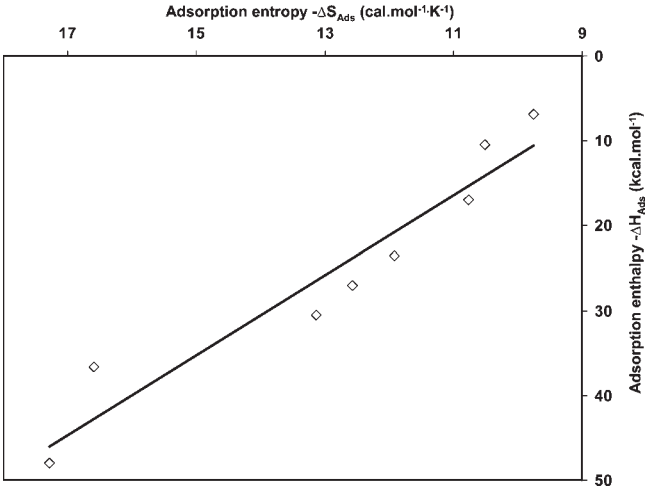

Figure 6. Linear correlation between the calculated adsorption entropy and enthalpy in MAZ.

Table 2. Calculated Confinement Compensation Temperatures a_j (10^3 K)[a]

frameworks	pore size (Å)	a (eq 5)	a (eq 14)
MAZ	10.1	4.7	5.2
AET	10.6	2.3	2.9
DON	10.8	2.3	2.8
FAU	14.5	1.9	2.7
VFI	15.4	1.2	1.5

[a] Relative errors for the determination according to eq 14 are 15% for MAZ and otherwise close to 10%; see Supporting Information, so that values determined by both methods do not differ significantly.

Analogous to ΔH_{ads}, the loss in entropy increases more quickly in smaller pores, since particles with a given V_m experience a greater loss in translational and rotational degrees of freedom. Unexpectedly, for MAZ, which has the smallest pore size, we calculate a slope that corresponds to those of FAU and VFI. This can likely be attributed to moderate statistics, even though the number of insertion steps had significantly been increased. Furthermore, these not so good statistics might also explain why the hosts do not have the same Y-intercept in common, when we extrapolate V_m to 0.

In addition, a linear correlation between the adsorption enthalpy and the adsorption entropy is observed with a positive slope that refers to confinement compensation temperature (a) as expressed in eq 5 (Figure 6). The confinement compensation temperature can either be determined using eq 5 or from eq 14. The results of both methods are presented in Table 2. It turns out that both manners do not converge to the same confinement compensation temperature; however, they are strongly correlated and are actually shifted by almost a constant value of 500 K. We attach more confidence to the confinement compensation temperatures calculated using eq 14, since both $a_{H,j}$ and $a_{S,j}$ result from a linear regression, while in eq 5 the confinement compensation temperature ensues from a "simple" linear regression from the individual values of ΔH_{ads} and ΔS_{ads} calculated for given molecular volumes.

The confinement compensation temperature is found to be dependent on the microporous framework and to decrease with increasing pore sizes: 5200 K for MAZ and 1500 K for VFI. This

dx.doi.org/10.1021/ja105950z |J. Am. Chem. Soc. 2011, 133, 2481–2491

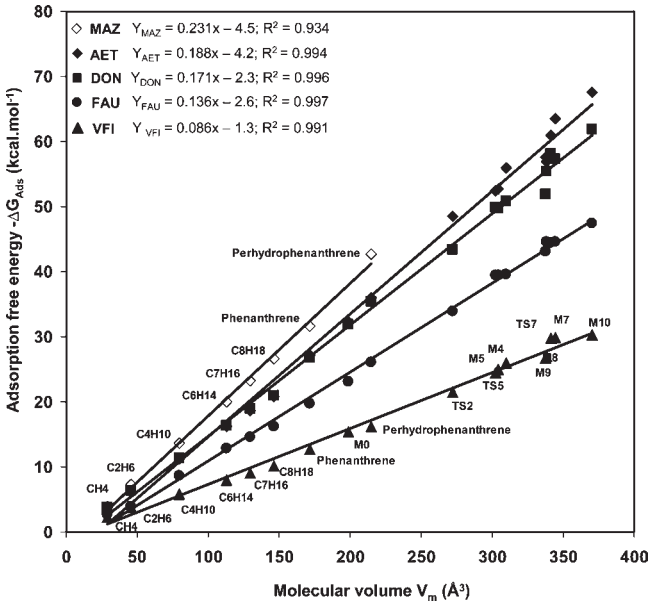

Figure 7. Calculated adsorption Gibbs free energies at 300 K as function of the molecular volume of the inserted species within the microporous structures: MAZ, AET, DON, FAU, and VFI.

tendency had already been observed for $a_{H,j}$ and $a_{S,j}$ and as well for $a_{G,j}$ (vida supra).

Figure 7 presents the adsorption Gibbs free energy at T = 300 K as a function of the molecular volume of the inserted species for the five studied microporous solids. It is seen that the change in Gibbs free adsorption energy decreases with increasing molecular volume and that this change is more pronounced with decreasing pore size of microporous structures.

We mention moreover that we have measured cross-correlations between several descriptors, including or not linear hydrocarbons in the test set, with the results given in Supporting Information, Tables SI5 and SI6. From these tables it is evident that linear correlations will be found also for adsorption enthalpies and entropies versus total molecular mass, element count (mostly carbon count) and shadow areas or lengths (only if linear hydrocarbons are included). This however does not force us to reconsider our choice of molecular volume to describe the confinement effect, as discussed in section 2.3 above.

4.2. Impact of Confinement on Oligomerization Activity and Selectivity. In this paragraph we show how confinement effects precisely impact the reaction rates and selectivities, using the confinement compensation temperatures and a_H (proportionality coefficient between the negative of adsorption enthalpy and molecular volume) previously calculated.

We have first to identify the effect of confinement on the localization of rate determining steps along each oligomer production pathway, with respect to the situation in the homogeneous phase. We now return to the notation of Figure 1 and ref 10 for intermediates and transition states, considering in sequence the growth steps M2→M5 via TS4, M5→M8 via TS7, M8→M10 via TS9, and the corresponding β-elimination steps producing α-hexene from M5 via TS5 and α-octene from M8 via TS8.

We report in Table 3 the coefficients C and D allowing to compute the temperature dependence of the free energy barriers for these steps in homogeneous phase, according to the linear expansion of eq 23.

Table 3. Coefficients of the Linear Expansions with Temperature (eq 23), of Free Energy Barriers in Homogenous Phase, Computed by DFT According to Methods Described in Ref 10

barrier	C (kcal·mol^{-1}·K^{-1})	D (kcal·mol^{-1})
M2→TS4 (expansion)	0.062	3.48
M5→TS5 (β-elimination)	0.005	16.78
M5→TS7 (expansion)	0.043	11.45
M8→TS8 (β-elimination)	0.004	12.24
M8→TS9 (expansion)	0.044	6.18

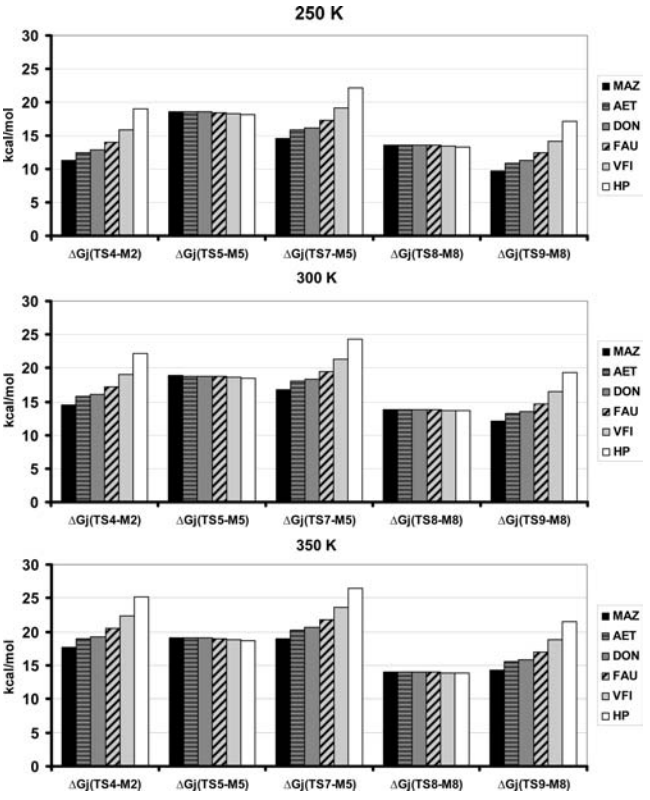

Figure 8. Computed free energy barriers as a function of temperature and confining host. HP stands for the homogeneous phase. Each bundle of bars stands for one step, with increasing oligomerization degree from left to right. Increasing confinement (from right to left in a bundle) affects growth steps significantly and β-elimination steps hardly.

Inserting in eqs 11 and 12 the coefficients $a_{H,j}$ obtained for each host structure (slope of Figure 4), the values a_j reported in Table 2 (from eq 14), and the values $b_{G,j}$ obtained at 300 K (inset of Figure.7), we have computed the values of $a_{G,j}$ at three temperatures: 250, 300, and 350 K. Using finally eqs 23 with the coefficients of Table 3 and eqs 20 and 21, we have computed the relevant free energy barriers at these temperatures, for the various host structures considered. The results are presented graphically in Figure 8.

From Figure 8, it appears first that the overall rds for the production of α-octene and beyond, is always the growth step M5→M8 via TS7 (third bundle of bars from left to right) whatever the temperature. In homogeneous phase (HP) and VFI at 250 K, HP, FAU, and VFI at 300 and 350 K, the corresponding barriers are higher than those for β-elimination from M5 via TS5, giving α-hexene. Following a similar pattern, the barriers for β-elimination

dx.doi.org/10.1021/ja105950z |J. Am. Chem. Soc. 2011, 133, 2481–2491

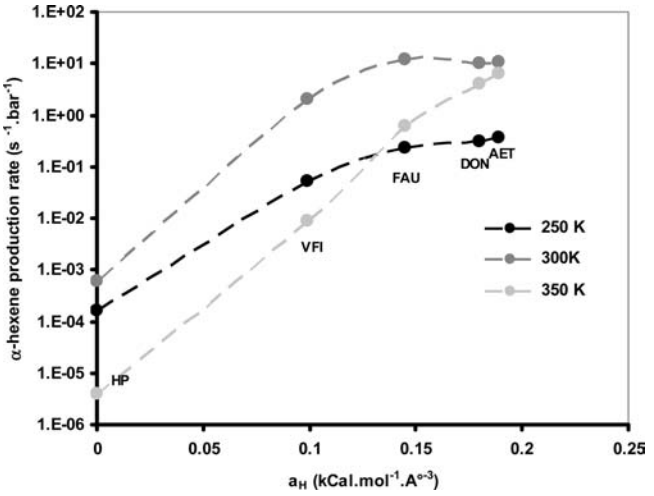

Figure 9. Effect of confinement described by $a_{H,j}$ on the rates of α-hexene production at 1 bar ethene pressure and T = 250 K (black), 300 K (dark gray), and 350 K (light gray). Symbols correspond to the predicted values. Interrupted lines are mere guides for the eye. HP stands for "homogenous phase" (a_H = 0).

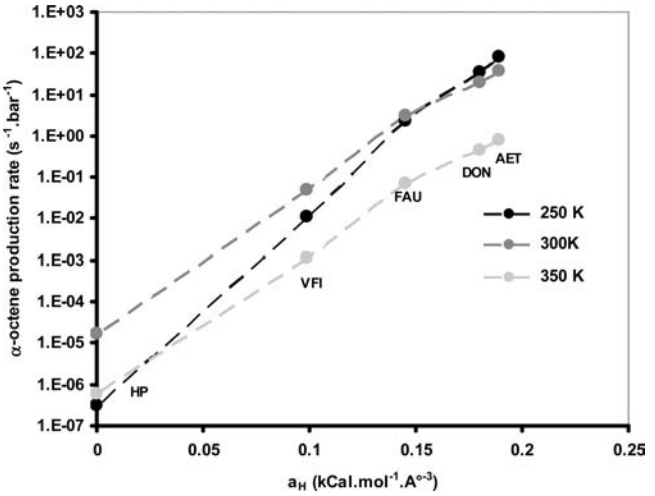

Figure 10. Effect of confinement described by $a_{H,j}$ on the rates of α-octene production at 1 bar ethene pressure and T = 250 K (black), 300 K (dark gray), and 350 K (light gray). Symbols correspond to the predicted values. Interrupted lines are mere guides for the eye. HP stands for "homogenous phase" (a_H = 0).

from M8 via TS8 giving α-octene are lower than that for growth M8→M10 via TS9. Therefore, no large amount of α-decene can be expected to be obtained upon confinement of the Teuben catalyst in VFI and FAU structures above 300 K. Confinement in structures MAZ, AET, and DON might allow pentamerization of ethene, provided M10 would not be sterically excluded: from our GCMC calculations, this is the case for MAZ, which does not accept even M2. We sit on the borderline for AET and DON, for which insertion acceptance probabilities are very small (10^{-6}) compared to that achieved for smaller intermediates, while FAU and VFI accept M10 with reasonable probabilities (10^{-3}). We conclude conservatively that N_{max} = 0 for MAZ and N_{max} = 4 for AET and DON.

Using eqs 18 to 25, taking into account the rds for each oligomerization pathway and the restraints to insertion discussed above, we have computed the effect of confinement on the oligomer production rates and selectivities at 250, 300, and 350 K, at 1 bar ethene pressure. Figures 9 to 11 present the predicted rates for α-hexene, α-octene, and α-decene productions. Figures 12 to 14 present the corresponding selectivities and Figure 15 the total oligomerization productivities.

From these figures, one notices first the striking effect of confinement predicted from our analysis: 5 to 7 orders of magnitude, depending on temperature, are spanned for the overall oligomerization rates. Two to three orders of magnitude in amplification are due to the sole confinement of ethene, the remaining effect being caused by the marked reduction in metallacycles growth free energy barriers induced by the corresponding differentials in molecular volumes.

This strong amplification in productivity goes with changes in selectivity toward higher oligomers than α-hexene, provided the corresponding intermediates and transition states are not excluded from the hosts. AET and DON would become selective in α-octene at ambient and subambient temperatures. At 350 K, the selectivity shifts back to α-hexene, while the overall productivity is still amplified by 5 orders of magnitude. An optimal temperature exists between 250 K and 350 K. The FAU structure is predicted to exhibit some selectivity in α-decene at 250 K, though it fades out rapidly with increasing temperature. The same tendency is observed for the more open (less confining) VFI structure.

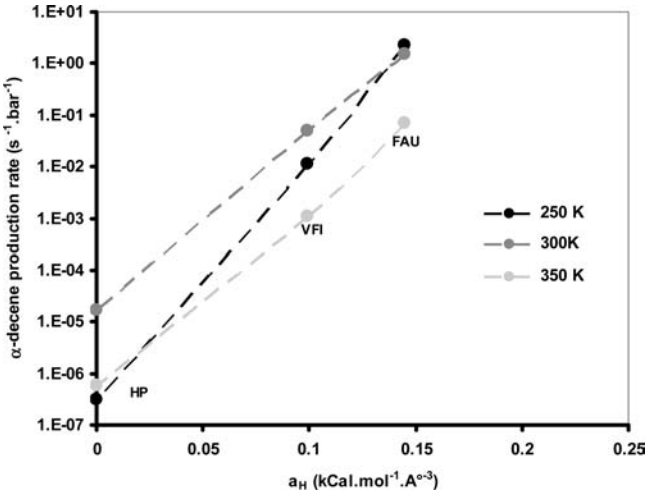

Figure 11. Effect of confinement described by $a_{H,j}$ on the rates of α-decene production at 1 bar ethene pressure and T = 250 K (black), 300 K (dark gray), and 350 K (light gray). Symbols correspond to the predicted values. Interrupted lines are mere guides for the eye. HP stands for "homogenous phase" (a_H = 0).

A detailed analysis of uncertainties affecting the predicted effect of confinement on confinement compensation temperature, rates, and selectivities is reported in Supporting Information. For the time being, we do not consider systematic errors that might arise from the particular choices we have made for the GCMC calculations (hosts and guests molecular model, forcefield, electrostatic effects neglected). Rather, we have evaluated how uncertainties propagate from the DFT calculations and the regression analysis performed on the GCMC calculation results. We find that rather large relative uncertainties may affect the prediction of absolute rates and selectivities. They become larger with decreasing host pore size. However, the relative uncertainties on relative rates remain moderate (10 to 20%) for the cases of interest (VFI, FAU, DON, AET). In other terms, assuming the rates in homogeneous phase are known exactly (e.g., experimentally),

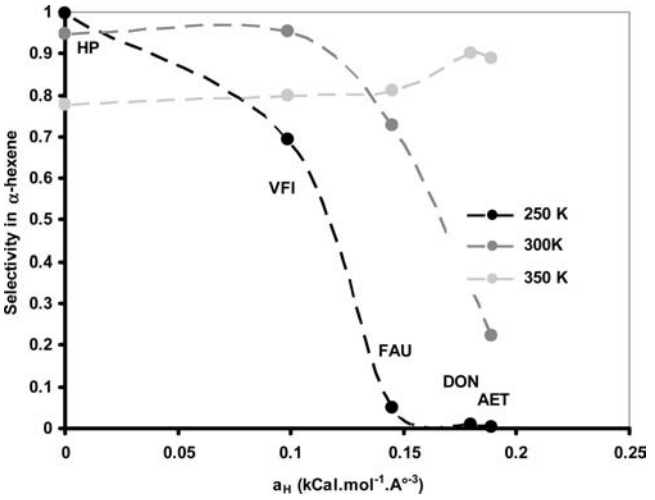

Figure 12. Effect of confinement described by $a_{H,j}$ on selectivity in α-hexene at 1 bar ethene pressure and T = 250 K (black), 300 K (dark gray), and 350 K (light gray). Symbols correspond to the predicted values. Interrupted lines are mere guides for the eye. HP stands for "homogenous phase" ($a_H = 0$).

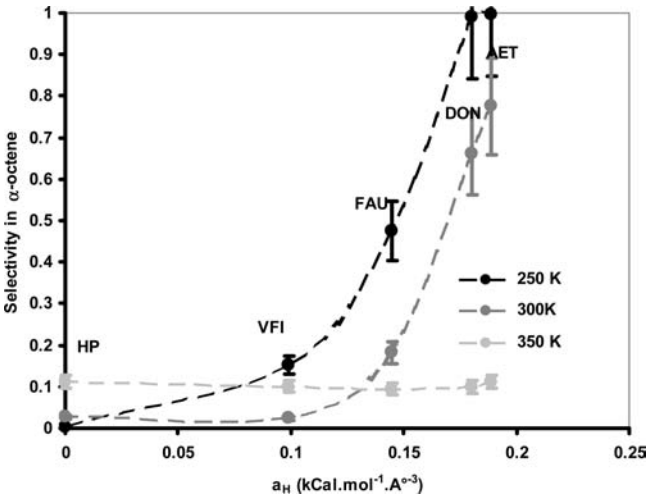

Figure 13. Effect of confinement described by $a_{H,j}$ on selectivity in α-octene at 1 bar ethene pressure and T = 250 K (black), 300 K (dark gray), and 350 K (light gray). Symbols correspond to the predicted values. Interrupted lines are mere guides for the eye. HP stands for "homogenous phase" ($a_H = 0$). (Error bars are placed according to the results of error calculations available in Supporting Information.)

the trends in accelerations induced by confinement are correctly predicted by our analysis.

In Figures 13 and 15 error bars have been placed on the log scale in ordinates and on the linear scale in abscissae as evaluated in Supporting Information. For the sake of clarity, we have avoided placing error bars on the other figures.

For the case studied, metallacyclic oligomerization catalyzed by the Teuben complex, the optimal confinement is therefore predicted to lie within a rather narrow window of pores sizes: pore should be large enough to accommodate intermediates and transition states, but not too large so that guests may be effectively stabilized by short-range attractive interactions with host pore walls.

Taking into account the above-presented results, to maximize α-octene production the oligomerization reaction should be

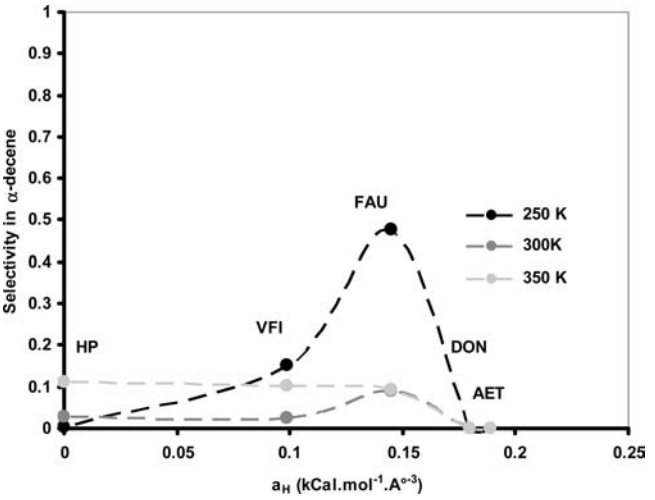

Figure 14. Effect of confinement described by $a_{H,j}$ on selectivity in α-decene at 1 bar ethene pressure and T = 250 K (black), 300 K (dark gray), and 350 K (light gray). Symbols correspond to the predicted values. Interrupted lines are mere guides for the eye. HP stands for "homogenous phase" ($a_H = 0$).

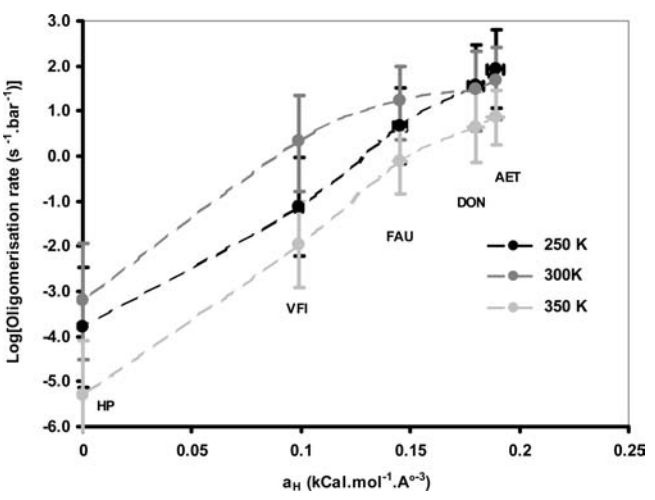

Figure 15. Effect of confinement described by $a_{H,j}$ on overall oligomerization rates at 1 bar ethene pressure and T = 250 K (black), 300 K (dark gray), and 350 K (light gray). Symbols correspond to the predicted values. Interrupted lines are mere guides for the eye. HP stands for "homogenous phase" ($a_H = 0$). (Error bars are placed according to the results of error calculations available in Supporting Information.)

conducted in microporous structure with a_H in the range 0.15−0.18 (like FAU, DON, AET) at relatively low temperatures (T < 300 K).

Of course, we are aware of some limitations of our model:

1 Our GCMC simulations treat guests as rigid bodies and hosts as rigid frameworks. Although these are rather crude approximations, we have chosen the conformations determined for energy minima or transition states by DFT. These geometries corresponded to quite steep energy minima. We assume that in the absence of guest/host specific interactions, the dispersive forces will not affect the guest geometries. Moreover, we have undertaken DFT calculations of the oligomerization profile confined in FAU supercages, at the quantum mechanics/molecular mechanics (QM/MM) level (electronic embedding with the ONIOM method).

dx.doi.org/10.1021/ja105950z |J. Am. Chem. Soc. 2011, 133, 2481–2491

Preliminary results confirm that rotations of the guests for instance affect the potential energy landscape by at most 2 kcal/mol, without noticeable changes in the stationary state geometries. This will be reported in a forthcoming manuscript. We expect therefore that the trends reported here within these rigid guest and host approximations will not change much, at least qualitatively, upon more sophisticated theoretical treatments.

2 Electrostatic interactions were neglected: this point has been already discussed in section 3.2. Forthcoming QM/MM results should again provide the state of the art complement on that point.

3 It is possible that oligomers production rates are in reality limited by mass transfer of reactant ethene or produced oligomers in microporous hosts. In the present report we have not attempted to predict such limitations. This will also depend on microporous host particle sizes. We leave that point for further research.

4 We have assumed that it is possible to activate the Teuben catalysts in presence of the cocatalyst (usually MAO) inside the host pores. This implies that a confined counteranion compensates for the positive charge borne by the molecular catalyst.

5. CONCLUSIONS

In this theoretical study we have shown that the activity and selectivity of a catalytic reaction outcome can be significantly altered by performing the catalysis in hosts with an adequate pore size, thereby optimizing host−guest van der Waals interactions, with respect to performing the reaction in a "traditional" homogeneous solution. As an example, we have noticeably shown that the selectivity of the oligomerization reaction of ethylene, catalyzed by a Ti-complex, may shift from α-hexene to α-octene or α-decene in a zeolitic framework like FAU as compared to homogeneous phase reaction in toluene.

With the use of GCMC calculations, we have calculated the Henry constants, Gibbs free energies of adsorption, adsorption enthalpies, and entropies for previously identified reaction intermediates in the tri/tetramerization reaction of ethylene in five different zeolitic frameworks where the pore diameter roughly ranges from 10.1 to 15.4 Å. Linear correlations are observed between the adsorption enthalpy and the molecular volume of the inserted guest molecule and between the adsorption entropy and the molecular volume of the guest molecule. The slopes $a_{H,j}$ and $a_{S,j}$ are host-dependent and are found to decrease as the pore size of the host structure increases. Moreover, since ΔH_{ads} and ΔS_{ads} appear linearly correlated, a confinement compensation temperature (a_j) can be defined. If reactions were run at this temperature in the microporous structure, the beneficial enhancement of adsorption enthalpies would be exactly canceled out by the loss in entropy. We have found that the confinement compensation temperatures decrease with increasing pore sizes from 5200 K ± 800 K for mazzite to 1500 K ± 150 K for VFI, but they remain much higher than the usual operating temperatures in catalysis.

With the use of $a_{H,j}$ and the confinement compensation temperature, reaction selectivities and activities can be calculated. The selectivity in α-octene formation increases with increasing $a_{H,j}$ values; however, when the pore size becomes too small, as in mazzite, the key transition state structure to form α-octene cannot enter anymore, since its molecular volume is too large with respect to available volume of the host. Additionally, it is concluded that α-octene and α-decene selectivities are negatively impacted by an increase in temperature.

From our calculations it follows that from the five zeolitic frameworks studied, MAZ, AET, DON, FAU, and VFI, the most promising host structures are AET, DON, and FAU to obtain the largest α-octene productivity in oligomerization reaction, run between −23 °C (250 K) and 25 °C.

Last but not least, we predict the possibility of very significant amplifications of the overall productivities in oligomers due to the combined effect of ethene confinement and intermediates and transition state confinement in the pores of adequate microporous hosts.

■ ASSOCIATED CONTENT

Supporting Information. (1) Derivation of eqs 8 to 10; (2) derivation of eqs 20 and 21; (3) constraints to rates of expansion and β-elimination in metallacyclic oligomerization; (4) estimation of errors on predicted rates and selectivities in confinement. Table SI5: coefficients of cross-correlation of various descriptors with molecular volume for the full set of molecular guests considered. Table SI6: coefficients of cross-correlation of various descriptors with molecular volume, for the set of molecular guests restricted to intermediates and transition state complexes involved in the oligomerization pathway. This material is available free of charge via the Internet at http://pubs.acs.org.

■ AUTHOR INFORMATION

Corresponding Author
herve.toulhoat@ifpenergiesnouvelles.fr

■ ACKNOWLEDGMENT

This work was supported by Award No. UK-C0017, made by King Abdullah University of Science and Technology (KAUST).

■ REFERENCES

(1) Li, C. *Catal. Rev.* **2004**, *46*, 419–492.
(2) Fink, G.; Steinmetz, B.; Zechlin, J.; Przybyla, C.; Tesche, B. *Chem. Rev.* **2000**, *100*, 1377–1390.
(3) Hlatky, G. G. *Chem. Rev.* **2000**, *100*, 1347–1376.
(4) Severn, J. R.; Chadwick, J. C.; Duchateau, R.; Friederichs, N. *Chem. Rev.* **2005**, *105*, 4073–4147.
(5) McMorn, P.; Hutchings, G. J. *Chem. Soc. Rev.* **2004**, *33*, 108–122.
(6) Zhao, X. S.; Bao, X. Y.; Guo, W.; Lee, F. Y. *Mater. Today* **2006**, *9*, 32–39.
(7) Sheldon, R. A. . In *Heterogeneous catalysis and fine chemicals II*; Guisnet, M., Barrault, J., Bouchoule, C., Duprez, D., Perot, G., Maurel, R., Montassier, C., Eds.; Elsevier Science Publishers B. V.: Amsterdam, 1991; pp 34−51.
(8) (a) Derouane, E. G.; Lucas, A. A.; Andre, J. M. *Chem. Phys. Lett.* **1987**, *137*, 336–340. (b) Derouane, E. G. *Chem. Phys. Lett.* **1987**, *142*, 200–204. (c) Derouane, E. G.; Andre, J. M.; Lucas, A. A. *J. Catal.* **1988**, *110*, 58–73.
(9) (a) Deckers, P. J. W.; Hessen, B.; Teuben, J. H. *Angew. Chem., Int. Ed.* **2001**, *40*, 2516–2519. (b) Deckers, P. J. W.; Hessen, B.; Teuben, J. H. *Organometallics* **2002**, *21*, 5122–5135.
(10) De Bruin, T. J. M.; Magna, L.; Raybaud, P.; Toulhoat, H. *Organometallics* **2003**, *22*, 3404–3413.
(11) Blok, A. N. J.; Budzelaar, P. H. M.; Gal, A. W. *Organometallics* **2003**, *22*, 2564–2570.

(12) Tobisch, S.; Ziegler, T. *Organometallics* **2003**, *22*, 5392–5405.
(13) McQuarrie, D. A.; Simon, J. D. *Molecular Thermodynamics*; University Science Books: Sausalito, CA, 1999; p 403.
(14) Masel, R. I. *Principles of Adsorption and Reaction on Solid Surfaces*, 1st ed.; John Wiley and Sons: New York, 1996; p 240.
(15) Campelo, J. M.; Garcia, A.; Luna, D.; Marinas, J. M. *J. Catal.* **1986**, *97*, 108–120.
(16) Ruthven, D. M.; Kaul, B. K. *Adsorption* **1998**, *4*, 269–273.
(17) Conner, W. C. *J. Catal.* **1982**, *78*, 238–246.
(18) Eyring, H. *J. Chem. Phys.* **1937**, *3*, 107–115.
(19) Baerlocher, Ch.; Meier, W. M.; Olson, D. H. *Atlas of Zeolite Framework Types*, 5th ed.; Elsevier: Amsterdam, 2001.
(20) Frenkel, D.; Smit, B. *Understanding Molecular Simulation. From Algorithms to Applications*; Academic Press: San Diego, CA, 1996; pp 126−135.
(21) Smit, B.; Siepmann, J. I. *J. Phys. Chem.* **1994**, *98*, 8442–8452.
(22) *Materials Studio*, version 4.4; Accelrys Software Inc.: San Diego, CA, 2009.
(23) Benazzi, E.; Leite, L.; Marchal-George, N.; Toulhoat, H.; Raybaud, P. *J. Catal.* **2003**, *217*, 376–387.
(24) Toulhoat, H.; Raybaud, P.; Benazzi, E. *J. Catal.* **2004**, *221*, 500–509.
(25) Hagen, H. *Ind. Eng. Chem. Res.* **2006**, *45*, 3544–3551.